Available online at www.sciencedirect.com
SCIENCE DIRECT®
Journal of Power Sources 148 (2005) 121–128
JOURNAL OF POWER SOURCES
www.elsevier.com/locate/jpowsour

Studies on nanoporous glassy carbon as a new electrochemical capacitor material

Yuehua Wen*, Gaoping Cao, Yusheng Yang

Research Institute of Chemical Defense, Beijing 100083, China

Received 18 August 2004; received in revised form 20 December 2004; accepted 1 February 2005
Available online 16 March 2005

Abstract

A nanoporous glassy carbon (NPGC) used as a new electrochemical capacitor material has been developed and prepared from a novolac phenolic resin. This new porous carbon has a high specific capacity due to its large surface area and a high power density due to its nice bulk conductivity and nanoporous structure. In this paper, main factors that influence the pore structure and electrochemical performance of NPGCs were systematically investigated. The results showed that the porosity of carbonized resin increased with curing temperature up to 225 °C at which the resin can be cross-linked fully, facilitating activation agent molecules to diffuse inward. It was also found that high carbonization temperature helped crystallization of carbonized products, but the shrinkage of carbon skeleton made the extent of activation decrease. Meantime, increasing activation temperature may accelerate reaction rate and prolonging activation time may increase the extent of activation. However, too high activation temperature and too long activation time can make the carbon matrix cracked and distorted. Therefore, a maximum capacity of 203 F g^{-1} and a conductivity of about 10 S cm^{-1} was obtained for the NPGC sample prepared under suitable conditions, resulting in high power densities (6.5 kW kg^{-1} carbon).

Keywords: Nanoporous carbon; Microstructure; Electrochemical properties

1. Introduction

Much interest has been focused on the application of carbon as electrode materials because of their accessibility, chemical stability and existence in a variety of structure [1]. So, at present activated carbon powders and activated carbon fiber cloths are widely used as electrodes for commercial electric double-layer capacitors (EDLCs) [2]. But, it is difficult for them to meet the demands for preparing high power EDLCs due to their high interparticle contact resistance.

Glassy carbon (GC) possesses good mechanical properties, high conductivity and low gas permeability with closed pores in the matrix [3]. Gas-impervious GC cannot be an excellent EDLC electrode material because it is unable to be activated totally. For example, in 1980, Miklos [4] used GC plates activated by air oxidation as polarized electrodes for EDLCs. But they only turned the GC surface into porous structure. At the end of the 1990s, activation of GC surface was also attained by electrochemical oxidation and a 1 V two-electrode capacitor with 2 F was built in Switzerland by Sullivan et al. [5–7]. Afterwards, they activated GC sheets with a thickness of only 55 um by thermal oxidation, and built a 5 V multicell bipolar stack with a power density of 32.6 kW L^{-1} [8–10]. The energy density of this stack was too low to be suitable for application. Recently, we applied potentiostatic oxidation to activate GC and found that although power characteristics of the active carbon layers were excellent, the thickness of active layers was limited and the specific capacitance of the whole GC was considerably low [11]. So far, there are some reports about porous GC, but their pore diameter is too large to be suitable for EDLCs [12,13]. So, we assumed that if closed pores were opened and nanoporous structure were established, GCs specific surface areas would be increased greatly and it potentially becomes an ideal carbon electrode for supercapacitors with high power density.

* Corresponding author. Tel.: +86 10 6674 8507; fax: +86 10 6674 8574.
E-mail address: wen_yuehua2002@yahoo.com.cn (Y. Wen).

0378-7753/$ – see front matter © 2005 Elsevier B.V. All rights reserved.
doi:10.1016/j.jpowsour.2005.02.001

The production of GC requires very slow cure and carbonization cycles, resulting in a very high cost [14,15]. To solve this problem, in 1971, Jenkins and Kawamura [16] developed a technique in Swansea for making disc GCs by using excess phenol in a phenol–hexamine system. This uncrosslinked polymer pre-treated to 300–330 °C was crushed into fine powder, compacted to a shape and was heated rapidly to complete its carbonization at 1000 °C in nitrogen. Then, GC discs with apparent between 1.35 and 1.5 g cm^{-3} can be obtained. This simple and quick method called "Swansea process" makes GCs preparation cycle shortened considerably.

In this paper, we report a novel electrode material, nanoporous glassy carbon (NPGC), for EDLCs and its preparation. The method for preparing the NPGCs was based on the grinding and compacting technique similar to "Swansea process". This allowed us to obtain a compacted resin with a desired porosity through which gaseous products were given off easily without destroying the original shape during carbonization and activation. Comparing with the "Swansea process", we added some hexamine into a novalac phenolic resin to make it hardened at temperatures below 300 °C. Some degree of cross-linking between polymer chains took place. Then a phenolic precursor with partial cure and its carbonized product with an open porosity were obtained. So, the carbonized matrix can be activated monolithically. The objectives of the current research include discussing the relationship between the electrochemical characteristics and main factors that affect the activation extent of NPGCs in detail, and reporting physical properties such as apparent density of the NPGCs and crystallinity of the carbonized resin along with capacitor performance.

2. Experiment

2.1. Materials preparation

The phenolic resin-based NPGC was prepared as follows: a novolac resin was mechanically mixed with 10 wt.% hexamethylene tetramine with a grinding machine. The mixture was cured by heating. The cured resin was ground into fine particles and compacted into a disc with a diameter of 20 mm and thickness of 0.8 mm under a stress of 380 MP. Then, the compacted resin disc was carbonized in N_2 at desired temperature for 30 min, followed by CO_2-activation of carbonized discs at desired temperature for different time to form NPGCs.

2.2. Microstructure characterization

A computer-controlled thermogravimetric analyser (TGA, Netzsch STA449c Simultaneous DTA-TGA, TA Instruments) was used to study the weight change during heating process. And a Dupont 1090B thermogravimetric analyser (TGA-951) and differential scanning calorimeter (DSC-951) was used to determine the thermal effects of the cured resins during pyrolysis in a N_2 atmosphere at a heating rate of 5 °C min^{-1}. An X-ray diffractometer (XD-3A, Shimato) equipped with a Cu target was used to characterize the crystalline structure of NPGCs carbonized products. The porosity p of the carbonized samples from their X-ray density ρ_x and their apparent density ρ_g by using the relation: $\rho_x = (3.33538/d_{(0\,0\,2)}) \times 2.268\ \mathrm{g\,cm^{-3}}$, $p = 1 - \rho_g/\rho_x$, where 2.268 g cm^{-3} is the density of graphite with $d_{(0\,0\,2)} = 3.33538$ Å.

Adsorption isotherms, surface area, and pore volume analysis were performed using the BET and BJH model by a Micromeritics Instrument Corporation ASAP 2010 using nitrogen adsorbate at 77 K.

2.3. Electrochemical characterization

To remove gas trapped within the pores of the NPGCs, electrode discs were immersed in 6 mol l^{-1} KOH and placed under vacuum for more than 10 h before electrochemical measurement. A testing capacitor was composed of two facing NPGC electrodes separated by a polypropylene film which was previously impregnated with 6 mol l^{-1} KOH. A foam nickel was used as a current collector. Electrochemical experiments of the capacitor were carried out by using an electrochemical test station (Solartron 1280B, England) at room temperature. Equivalent series resistance (ESR) was measured at 1 kHz at 1 bias. Galvanostatic charge/discharge equipment (LX PCBT-128D-D, Wuhan) was employed to perform charging and discharging experiments. The voltage limits were set between 0 and 1 V. The dc capacitance (C) of a single NPGC electrode was calculated through the following formula:

$$C = 2It/\Delta Vm$$

where I is the discharge current, t the discharge time, ΔV the potential change on discharge and m is the mass of a electrode. Each cell was cycled 30 times. The conductivity was measured via a four-probe method.

3. Results and discussion

3.1. Curing

In this paper, the novolac phenolic resin was mechanically mixed with a hardener in solid phase. There exists an interface between two reagents. So, the curing temperature must be higher than 150 °C [17]. Because the hexamine starts to sublimate at 230 °C, the effect of solidification temperature on the structure and properties of the NPGCs was studied in detail from 150 to 250 °C.

Physical properties of the products formed by pyrolysis of phenolic resins cured at different temperature are presented in Table 1. It can be seen that the resin cured at 150 °C had the

Table 1
Physical properties of phenolic resin cured at different temperature and carbonized at700 °C

Solidification temperature (°C)	Weight loss of curing (%)	Carbon yield (%)	Diameter shrinkage (%)	Height shrinkage (%)[a]	Apparent density (g cm^{-3})
150	7.16	64.75	17.0	5.6	1.20
200	9.17	55.64	19.6	3.1	1.04
225	9.69	56.30	16.8	−8.7	0.83
250	11.14	55.73	17.4	−11.8	0.76

[a] A positive value of height means a decrease in height and a negative value means an increase in height.

lowest weight-loss during curing and its carbon yield is the highest. For the samples cured at temperatures above 200 °C, their carbon yields were lower. With increasing curing temperature, the densities of carbonized products decreased gradually due to the different extent of shrinkage, indicating an increase in the porosity of carbonized products.

To explain the above phenomena, the thermal characteristics of typical resins cured at 150 and 250 °C were studied with TGA and DSC, respectively. The results are shown in Fig. 1. It indicates that only a total weight loss of about 38% during pyrolysis in N_2 for the resin cured at 150 °C is observed. The 7% of the initial weight loss occurred before 400 °C probably due to the desorption of moisture, the major weight loss between 400 and 600 °C, a little weight loss occurred above 600 °C. In the same plot, the DSC signal shows only a high and narrow peak for exothermic effects, indicating that chemical condensation reactions and cyclizations take place. Whereas, for the resin cured at 250 °C, a total weight loss is beyond 55%. But, the first weight loss occurred before 400 °C is only 3% probably due to the higher degree of crosslinkage. Above 400 °C the weight loss considerably increased probably because it is more difficult for the cured resin with well cross-linked structure to cyclize in the pyrolysis, leading to more low molecular weight compounds released. The corresponding DSC curve exhibits a low and wide peak for exothermic reactions. In addition, the release of a large number of pyrolysed compounds may result in an expansion between carbon particles and an increase in thickness.

In order to further optimize pore structure and enlarge accessible surface area, the carbonized resin was activated in flowing CO_2 at 900 °C for 15 min. The measured pore structure data of activated products are presented in Table 2. It was observed that the specific surface area and pore volume increased with curing temperature up to 225 °C, above which they changed little. Fig. 2 illustrates the variation of the specific capacitance of the NPGCs prepared from cured resins at different temperatures with charge–discharge current and Fig. 3 gives their electrochemical impedance spectra (EIS) plots.

It was found that the NPGCs prepared from the resin cured at 150 °C cannot be used as electrode materials for supercapacitors due to its very low capacity and poor impedance characteristics. Cured at 200 °C, the activated sample's specific capacitance is as high as 159 F g^{-1} at small current density. But its capacity falls sharply with increasing charge–discharge current density. As shown in its EIS plot (Fig. 3), a bias of 45° appears at higher frequency indicating that the concentration-difference polarization is serious. As shown in Fig. 1, the samples cured at temperatures above 225 °C displayed very similar discharging characteristics with a specific capacitance of about 170 F g^{-1} at small current density and remarkable improvement on the large charge–discharge current behavior. Their EIS plots in Fig. 3 show that the imaginary part of impedance is apparently reduced and the capacitive behavior begins to appear at low frequency. Therefore, the curing temperature should be above 225 °C.

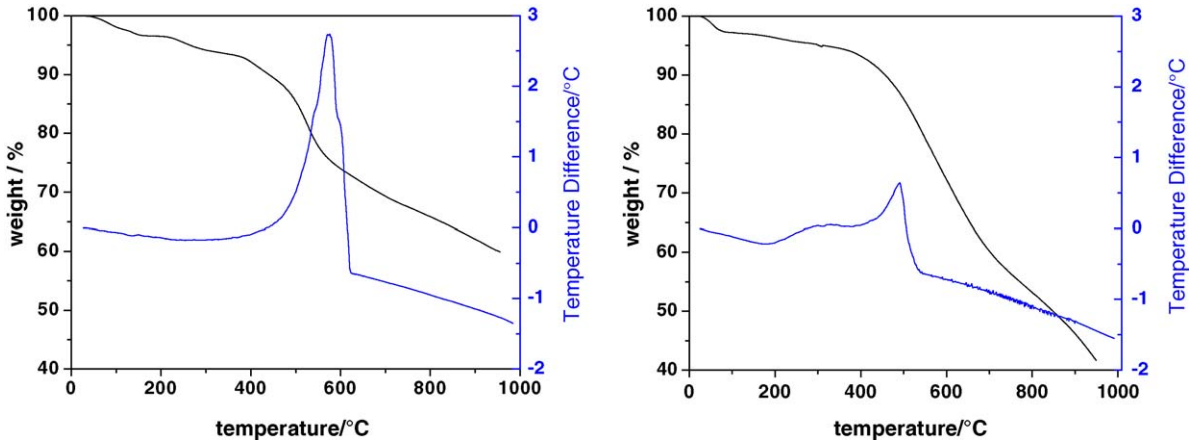

Fig. 1. The TGA/DTA curves of cured phenolic resin at 150 and 250 °C during pyrolysis.

Table 2
Effect of solidification temperature on pore structure of nanoporous glassy carbon

Solidification temperature (°C)	Burn-off of activation (%)	S_{BET} ($m^2\ g^{-1}$)	S_{mic} ($m^2\ g^{-1}$)	V_{tot} ($cm^3\ g^{-1}$)	V_{mic} ($cm^3\ g^{-1}$)	V_{mes} ($m^3\ g^{-1}$)[a]
150	5.6	235	203	0.13	0.094	0.04
200	12.9	825	727	0.42	0.34	0.08
225	12.6	891	798	0.44	0.37	0.07
250	13.9	876	793	0.44	0.37	0.07

[a] $V_{mes} = V_{tot} - V_{mic}$.

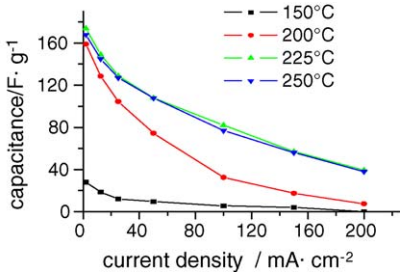

Fig. 2. Change of specific capacitance of NPGC obtained from resin cured at different temperature with charge–discharge current density.

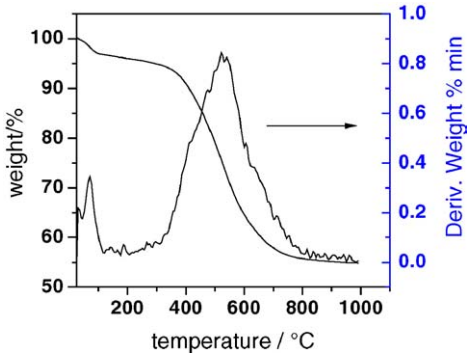

Fig. 4. TGA of compacted phenolic resin discs in N_2 at a temperature scan rate of 5 °C min^{-1}.

3.2. Carbonization

TGA of the cured phenolic resin is shown in Fig. 4, which indicates that there is a slight weight loss before 300 °C corresponding to the removal of retained water. The weight decreased continuously from 300 to 700 °C, especially from 400 to 600 °C because most chemical decomposition reactions of the material take place in this temperature rang. Above 700 °C, there is only a little of hydrogen to be released. Therefore, little weight loss was exhibited, indicating only structural changes are taking place [19]. So, we decided to investigate the influence of carbonization temperature on activation and features of the NPGCs between 600 and 1000 °C.

Table 3 displays the property data of the NPGCs obtained by carbonization at different temperatures and activation in flowing CO_2. It can be seen that as carbonization temperature increased from 600 to 700 °C, the carbon yield dropped significantly. But above 700 °C, the yield differs slightly. This is consistent with TGA results. Moreover, the burn-off of activation and specific capacitance of the samples gradually decreased with increasing carbonization temperature. However, the conductivity continuously increased.

An explanation for this phenomenon is proposed based on the X-ray diffraction (XRD) patterns (Fig. 5) and porosity of carbonized resins treated at temperatures ranging from 600 to 1000 °C (Fig. 6). The XRD profiles of compacted resins show only a broad and relatively symmetric peak at a scattering angle of about 20°. After heat treatment at 500 °C, the diffraction profile is similar to that of the untreated resin except for a peak at 43° observed, suggesting that the extent of carbonization is low. After pyrolysis at 600 °C, the peak corresponding to d_{002} becomes wider due to the structure reforming. After pyrolysis above 600 °C, the peaks corresponding to d_{002} and d_{100} spacings become narrow somewhat and shift to higher angles with increasing carbonization temperature. Meantime, a new peak appears at about 80°, indicating that the crystallite dimensions increase and the structure of carbonized resins becomes more ordered with an increase in conductivity. Therefore, when phenolic resin is carbonized at low temperatures, the pyroresin is most susceptible to activation with high burn-off and specific capacitance. On the contrary, carbonized at high temperatures, carbon skeleton shrinks, leading to a decrease in porosity and a more ordered structure. As a consequence, the activation process is diffusionally controlled, lowering

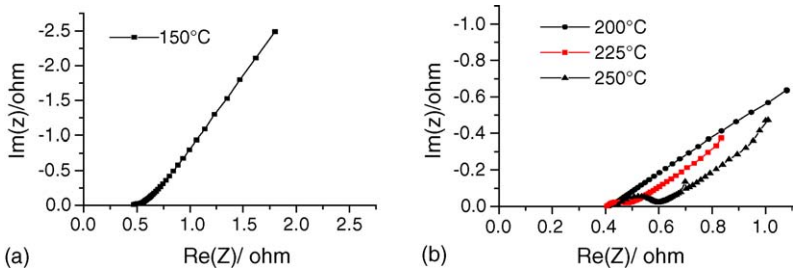

Fig. 3. Electrochemical impedance spectra of NPGCs obtained from resins cured at 150 °C (a) and above 200 °C (b), 20 kHz to 0.1 Hz.

Table 3
Effect of carbonization temperature on the properties of NPGCs

Carbonization temperature (°C)	Yield (%)	Burn-off of activation (%)	Capacitance (F g^{-1})	Conductivity (S cm^{-1})	ESR (Ω cm^2)
600	59.1	16.2	190	4.3	0.886
700	56.5	16.0	194	6.3	0.968
800	55.3	12.5	179	7.0	0.858
900	54.9	7.5	162	10.7	0.634
1000	54.5	7.8	158	11.9	0.666

Activated at 900 °C for 15 min. Electrode: $\Phi 16 \times 0.7$ mm.

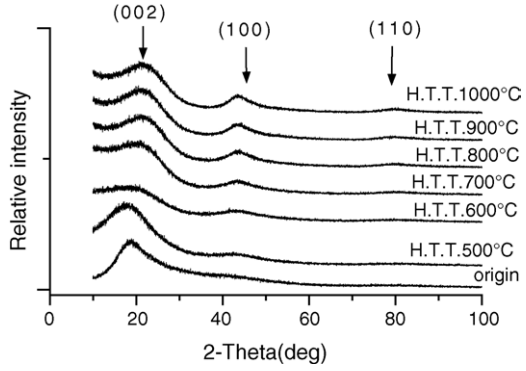

Fig. 5. XRD patterns of phenolic resin carbonized at different temperatures.

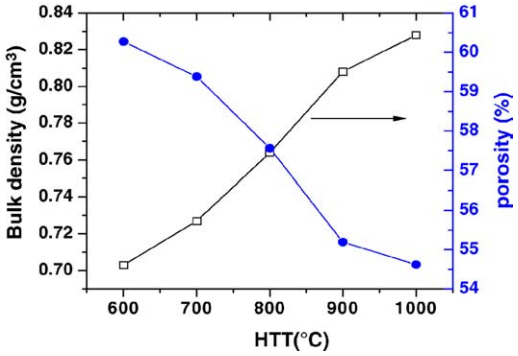

Fig. 6. Variation of apparent and porosity of resin carbon with carbonization temperature.

the reactivity. Thus, the burn-off and specific capacitance decrease.

The conductivity and pore structure of electrode materials are leading factors to affect the resistance of EDLCs. Furthermore, there is a close relationship between the specific capacitance and pore structure. Fig. 6 shows that the apparent density continues to increase, whilst the porosity decreases gradually with increasing carbonization temperature. The porosity of the carbonized product at 900 °C is about 55%, suggesting that diffusional inhibition of the oxidation reaction is still low. So, the NPGCs specific capacitance is high and conductivity is nice with the lowest ESR. From the standpoint of comprehensive properties, the proper carbonization temperature should be 900 °C.

3.3. Activation

The reaction between carbon and CO_2 can be accelerated by increasing temperature with a porosity raised. It can be seen from Table 4 that the burn-off of carbonized resins increases rapidly with increasing activation temperature leading to an increase in NPGCs specific capacitance. In contrast, their apparent density and conductivity continue to decrease. When the activation temperature was up to 975 °C, the carbonized matrix was activated excessively leading to a tremendous decrease in its mechanical intensity, and thus cracks appeared. Therefore, activated at 925 °C, the NPGCs specific capacitance was relatively high and its conductivity (about 12 S cm^{-1}) was also nice with the lowest ESR. The proper activation temperature should be 925 °C.

Table 5 shows that even when the carbonized resin is not activated, its apparent density is 0.75 g cm^{-3}, much lower than that of glassy carbon (1.5 g cm^{-3}). This indicates that the carbonized resin already has some porosity. With the extending of activation time, the burn-off increased significantly, resulting in an increase in specific capacitance and a decrease in apparent density and conductivity of the NPGCs. When the activation time was prolonged to 45 min, the skeleton of carbon matrix had been destroyed and cracks and distortion appeared. So, the activation time should be confined in 30 min under the above conditions.

Porosity measurements have been carried out in order to obtain basic information on the pore structure of the NPGCs

Table 4
Effect of activation temperature on the properties of NPGCs

Activation temperature (°C)	Burn-off (%)	Apparent density (g cm^{-3})	Capacitance (F g^{-1})	Conductivity (S cm^{-1})	ESR (Ω cm^2)
850	4.19	0.70	152	15.95	0.656
875	7.16	0.69	164	15.90	0.706
900	9.98	0.66	170	14.02	0.718
925	11.80	0.58	182	11.62	0.496
950	17.83	0.53	198	5.82	0.870
975	Fracture				

Electrode: $\Phi 16 \times 0.7$ mm.

Table 5
Effect of activation time on the properties of NPGCs

Activation time (min)	Burn-off (%)	Apparent density (g cm^{-3})	Capacitance (F g^{-1})	Conductivity (S cm^{-1})	ESR (Ω cm^{2})
0	0	0.75	130	16.54	0.982
15	11.80	0.62	182	11.62	0.496
30	18.39	0.58	203	10.47	0.420
45			Fracture		

Electrode: $\Phi 16 \times 0.7$mm.

Table 6
Effect of activation time on pore structure of phenolic resin-based nanoporous glassy carbon

Activation time (min)	S_{BET} (m^2 g^{-1})	S_{mic} (m^2 g^{-1})	V_{tot} (cm^3 g^{-1})	V_{mic} (cm^3 g^{-1})	V_{mes} (m^3 g^{-1})[a]
0	532	489	0.25	0.23	0.02
15	935	843	0.46	0.39	0.07
30	1379	1198	0.68	0.56	0.12

[a] $V_{mes} = V_{tot} - V_{mic}$.

activated for different time. As can be seen from Table 6, the unactivated sample not only has a low specific surface area and total pore volume, but also has a very low proportion of mesopores. After activated for 15 and 30 min, a marked increase in specific surface area and total pore volume were observed. Although their specific capacitance increased, it was not proportionally dependent on the BET surface. This suggested that some of micropores might have not contributed to the capacitance. It has been demonstrated in the literatures [18–21] that too small micropores are ineffective in forming the double-layer capacitance.

The N_2 adsorption isotherms at 77 K are shown in Fig. 7(a) for the three samples. The shape of these isotherms indicates type I isotherm which is typical for microporous carbon. The longer the activation time, the greater the amount of adsorption is. But a little adsorption hysteresis loop appeared with an increase in activation time, suggesting an increasing proportion of mesoporous volume. This can also be demonstrated from the mesoporous size distribution in Fig. 7(b). The pore sizes of the three samples are basically

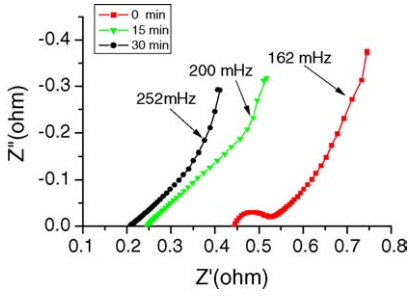

Fig. 9. The EIS plots for two electrode cells with a electrode area of 2 cm^2 containing samples obtained by CO_2-activation for different time.

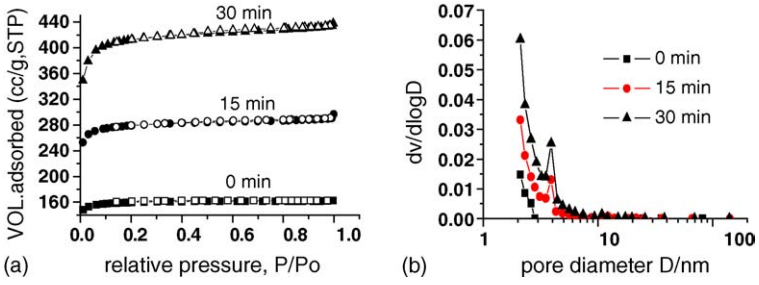

Fig. 7. N_2 adsorption isotherms at 77 K (a) of mesopore size distribution (b) of NPGCs obtained by CO_2-activation for different time.

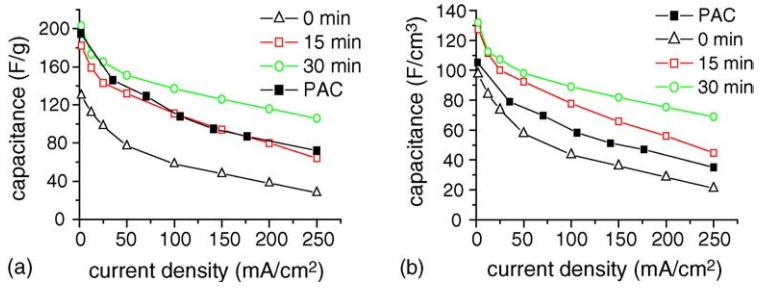

Fig. 8. Variation of the specific galvanostatic (a) and volumetric (b) capacitance with charge–discharge current density for NPGCs obtained by CO_2-activation for different time and comparison with PAC.

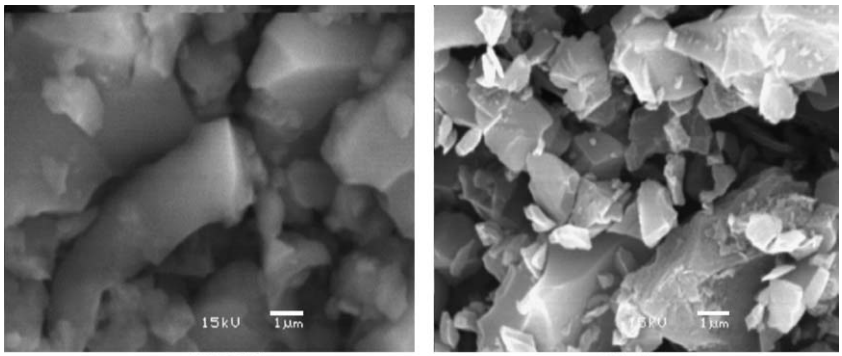

Fig. 10. SEM photographs of the NPGC activated for 30 min and PAC for comparison.

below 10 nm. The unactivated sample only exhibits a low peak with a mean pore width of about 2 nm which increases rapidly with activation time. Meantime, a new peak with a pore width of 4 nm appears and grows with activation time.

In the testing capacitor, a large charge–discharge current behavior and EIS for the three samples were studied. Fig. 8 shows the relationship between specific capacitance of the test electrode and the charge–discharge current density and comparison with the binder-used activated carbon (PAC) prepared from phenolic resin by CO_2-acitvation at the same experimental condition. The specific capacitance of the sample activated for 30 min was much higher than that of other samples under a high charge–discharge rate because of a higher surface area and a bigger mesoporous volume, facilitating the electrolyte ion to move quickly in pores. Although the specific gravimetric capacitance of PAC decreased with charge–discharge current density at the same rate as the sample activated for 15 min, the specific volumetric capacitance of PAC was much lower than that of activated NPGC samples with higher apparent density. Indeed, for application of electrochemical capacitors, the specific volumetric capacitance of electrode materials is of importance.

Fig. 9 presents the EIS plots for two-electrode cells with a electrode area of 2 cm^2. It can be seen that the real resistance was large for the unactivated sample, which decreased greatly with prolonging activation time. In high frequency region, the unactivated sample showed the presence of a loop. This loop was described as a pseudo-transfer resistance and shifted the appearance of capacitive behavior towards the high value of real resistance and the lower frequency. But this loop almost disappeared with prolonging activation time. For the sample activated for 30 min, it had more mesopores, hence increasing the pore accessibility. Its capacitive behavior appears at the low resistance and the higher frequency. The maximum power is obtained by

$$P_{max} = V^2/4R$$

the total resistance of the model capacitor was equal to its ESR, which was 0.21 Ω. Using a reasonable maximum voltage of 1 V (limited by the decomposition of water), a maximum power density of 6.5 kW kg^{-1} carbon can be obtained.

This EIS study further confirmed the results obtained by the galvanostatic charge–discharge cycling. It seems that for NPGCs with excellent conductivity, proper porous structure and high mesoporous percentage allow a good electrolyte penetration inside the electrodes, which become an important factor to determine the resistance and performance of charge–discharge rate.

The SEM images of the sample obtained by CO_2-activation for 30 min and comparison with PAC were shown in Fig. 10. It can be seen that carbon particles of the NPGC sample are piled tightly with some small pores, while PAC powders are in stack loosely with large pores.

4. Conclusions

The NPGC was prepared from a novalac phenolic resin through curing, grinding, compacting, carbonizing by fast heating and activating by CO_2. Overall, this study showed that as for the pore structure improved by CO_2-activation, the porosity of carbonized products increased with increasing curing temperature up to 225 °C, facilitating activation agent molecules to diffuse inward. Moreover, high carbonization temperatures helped crystallization of carbonized products, enhancing the conductivity. But the shrinkage of carbon skeleton made it difficult for activation agent molecules to diffuse inward so that the extent of activation and porosity could be reduced. Meantime, increasing activation temperatures may accelerate the reaction rate and prolonging activation time may increase the extent of activation with an increase in number of both micropores and mesopores. However, too high activation temperature and too long activation time can make the carbonized matrix cracked and distorted. This means that the phenolic resin-derived NPGCs cannot be activated excessively yet under current conditions. Therefore, the relatively optimal preparing conditions are as follows: a phenolic resin should be cured at 225 °C, and carbonized at 900 °C for 30 min, followed by CO_2-activation at 925 °C for 30 min to form NPGCs. Then the NPGC sample with a maximum capacity of 203 F g^{-1} and a conductivity of about 10 S cm^{-1} was obtained. The resistance of its

testing capacitor is low and its specific capacitance decreases slowly with charge–discharge current density, showing good performance of charge–discharge rate. This characteristics permit stored energy to be released rapidly, resulting in high power density (6.5 kW kg^{-1} carbon).

Acknowledgements

The authors wish to thank Academician Y.Sh. Yang for his serious-minded instruction in this study and permission to publish this paper, and Dr. G.P. Cao, Dr. J.Chen for their encouragement and help. Moreover, we are very grateful to the National Project 863 of China (No. 2002AA302405) for the financial support.

References

[1] K. Kinoshita, X. Chu, Electrochemical capacitors II, in: F.M. Delnick, M. Tomkiewicz (Eds.), The Electrochemical Society Proceedings Series, Pennington, NJ, USA, 1996, p. 171.
[2] S.T. Mayer, R.W. Pekala, J. Electrochem. Soc. 140 (1993) 446.
[3] G.M. Jenkins, K. Kawamura, Nature 231 (1971) 175.
[4] J. Miklos, Germany Patent 3,011,701.
[5] M.G. Sullivan, R. KÖtz, O. Haas, Electrochemical capacitors II, in: F.M. Delnick, M. Tomkiewicz (Eds.), The Electrochemical Society Proceedings Series, Pennington, NJ, USA, 1996, p. 198.
[6] M.G. Sullivan, M. Bärtsch, R. KÖtz, Electrochemical capacitors II, in: F.M. Delnick, M. Tomkiewicz (Eds.), The Electrochemical Society Proceedings Series, Pennington, NJ, USA, 1997, p. 192.
[7] M.G. Sullivan, B. Schnyder, J. Electrochem. Soc. 147 (2000) 2636.
[8] M. Bartsc, R. KÖtz, A. Braun, Proceedings of the 38th Power Sources Conference, Cherry Hill, NJ, 1998, p. 17.
[9] A. Braun, M. Bartsch, Materials, in: D.H. Doughty, L.F. Nazar, M. Arakawa, H.P. Brack, K. Naoi (Eds.), Research Society Symposium Proceedings, vol. 575, 2000, p. 369.
[10] A. Braun, M. Bartsch, J. Non-Cryst. Solids 260 (1999) 1.
[11] Y.H. Wen, G.P. Cao, J. Chen, Y.S. Yang, Chin. J. Power Sources 27 (2003) 455.
[12] Showa, Japan Patent 58,204,810.
[13] S. Kiyoshi, K. Masato, J. Takeshi, Japan Patent 10,072,266.
[14] E. Fitzer, W. Schaefer, S. Yamad, Carbon 7 (1969) 643.
[15] G. Bhatia, R.K. Aggarwal, M. Malik, O.P. Bahl, J. Mater. Sci. 19 (1984) 1022.
[16] G.M. Jenkins, K. Kawamura, Polymer carbon–carbon fiber glass and char, 1st ed., Cambridge University Press, Cambridge, UK, 1976.
[17] X. Liu, X.J. Hu, Y. Liu, Carbon Tech. 3 (1997) 12.
[18] J. Gamby, P.L. Taberna, P. Simon, J.F. Fauvarque, J. Power Sources 101 (2001) 109.
[19] C. Lin, J.A. Ritter, Carbon 38 (2000) 849.
[20] G. Salitra, A. Soffer, L. Eliad, Y. Cohen, D. Aurbach, J. Electrochem. Soc. 147 (2000) 2486.
[21] S. Shiraishi, H. Kurihara, L. Shi, T. Nakayama, A. Oya, J. Electrochem. Soc. 149 (2002) 855.